Adiabatic, Evaporating, Two-Phase Flow of Steam and Water in Horizontal Pipe

RALPH W. PIKE and HENDERSON C. WARD

Georgia Institute of Technology, Atlanta, Georgia

The adiabatic, evaporating, two-phase flow of steam and water in horizontal pipe including the critical flow was successfully described by a system of nonlinear differential equations which include different phase velocities, fluid acceleration, wall shear forces, interface shear forces, and mass and energy transfer between the phases. The solution of the differential equations by the method of Runge-Kutta was facilitated with a high-speed digital computer. Experimental data were obtained which included void fraction measurement by X-ray attenuation and showed that the theoretical equations described the complex flow phenomena to ± 10% when radial temperature gradients were small. Design charts based on the numerical solution of the theoretical equations are presented for rapid evaluation of the flow variables for the system steam-water including critical flow for inlet pressures from 30 to 150 lb./sq.in.abs., mass flow rates per unit area from 300 to 1,000 lb./sq. ft. sec., and L/D ratios from 25 to 1,000. The critical flow is defined as the maximum flow rate for a given pressure at the point of initial vaporization and L/D ratio.

Wide interest in two-phase flow is indicated by the abstracts and summaries given in the literature surveys by Gresham et al. (*1*), Ward et al. (*2*), Isbin et al. (*3*), and Bennett (*4*). Even with this large technical endeavor the methods to evaluate two-phase flow variables are generally empirical in nature and lend little incite to the flow mechanism. The two generally accepted methods of evaluating the flow parameters for adiabatic, evaporating flow of a pure fluid are the Martinelli-Nelson method (*5*) and the homogenous flow model (*6*). The accuracy of these two methods is generally of the order of ± 40%.

The Martinelli-Nelson method is an extension of the correlation of Lockhart and Martinelli (*7*) for the two-phase flow of air and various liquids to the flow of boiling water. This method has found wide acceptance as it correlates two-phase flow data over a wide range within reasonable limits.

The homogenous flow model derived its name from the fact that the basic assumptions of the model were that the liquid and its vapor flowed at the same average velocity, and that the physical properties of the fluid could be taken as an average of those of the liquid and the vapor. Benjamin and Miller (*6*) developed this model to describe the flow of steam and water in cascade drain lines. It has proved valuable as an additional way to estimate two-phase flow parameters by a straightforward calculation.

Although not in general use a third model, the Linning model (*8*), has included more of the flow variables than any previous model. In this model Linning included different phase velocities, mass acceleration, mass and energy transfer between the phases, interface shear forces, and wall shear forces. Linning found that he obtained excellent experimental verification of his theoretical equations over a limited range for the system of steam and water. However the notable disadvantages to the use of this are that a tedious numerical solution of the differential equations is required and a boundary condition at some point in the two-phase flow is necessary.

Other flow models have been presented in the literature. Some of these models are modifications of the Martinelli-Nelson model; some are modifications of the homogenous flow model, and some are referred to as *mixed* models (*3*), that is combinations of the Martinelli-Nelson and homogenous flow models. These models have had only slightly better success in describing the two-phase flow variables than the original ones. For discussions of flow models refer to the previously mentioned literature surveys and the surveys of Charvonia (*9*), Jens and Leppert (*10*), and Rodabaugh (*11*).

R. W. Pike is with the Humble Oil and Refining Company, Baytown, Texas.

DERIVATION AND SOLUTION OF THE ANNULAR FLOW EQUATIONS

To describe the adiabatic, evaporating, two-phase flow of a pure fluid the continuity, momentum, and energy equations are written in the manner suggested by Linning (*8*) based on the following assumptions:

1. The pipe is of constant cross-sectional area and is horizontal.
2. Steady state conditions exist.
3. The mean velocity of each phase is the same whether derived on the basis of continuity, momentum, or energy. (This does not mean that the velocities of the phases are equal.)
4. The pressure and temperature are constant across any section normal to the flow.
5. The fluid is near thermodynamic equilibrium at all stages in the expansion.

In Figure 1 a diagrammatic sketch of a section of fluid is given during annular flow. Referring to Figure 1 and considering the liquid and the vapor in the differential element as control volumes separately, one can derive the following equations on the basis of continuity and of the conservation of momentum and energy.

Continuity:

Liquid

$$W(1-x)v_l = a_l V_l \tag{1}$$

Vapor

$$Wxv_g = a_g V_g \tag{2}$$

Momentum:

Liquid

$$W(1-x)dV_l + a_l dP - \cos\theta\, dF_p + dF_w = 0 \tag{3}$$

Vapor

$$WxdV_g + W(V_g - V_l)dx + a_g dP + \cos\theta\, dF_p = 0 \tag{4}$$

Energy:

Liquid

$$W\Delta H dx + W(1-x)dh + W(1-x)V_l dV_l - V_p dF_p = 0 \tag{5}$$

Vapor

$$WxdH + WxV_g dV_g + 1/2(V_g^2 - V_l^2)Wdx + V_p dF_p = 0 \tag{6}$$

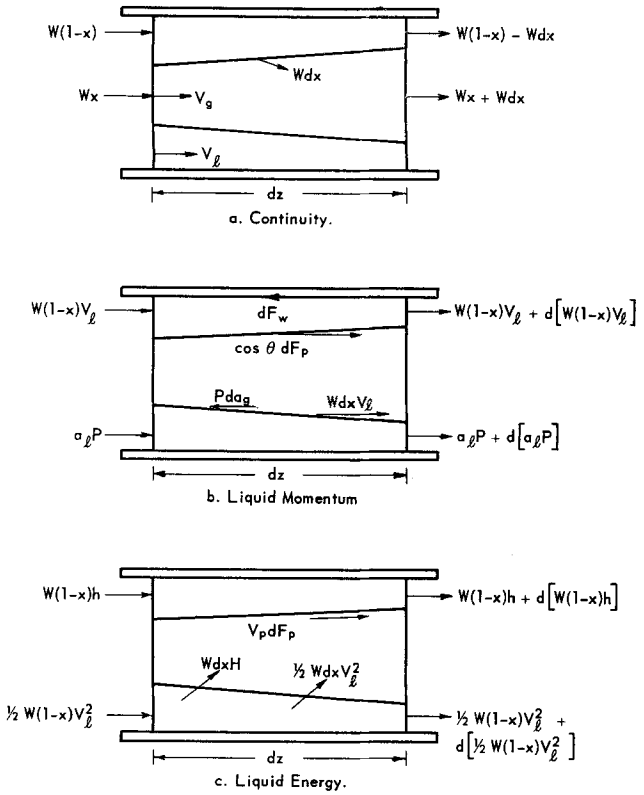

Fig. 1. Diagrammatic sketch of a section of fluid during annular flow.

The total energy equation is obtained by adding Equations (5) and (6). If this equation is integrated from the point of initial vaporization to any point downstream and the resulting equation is solved for the quality x, the result is

$$x = \frac{h_o - h + 1/2\,(V_o^2 - V_l^2)}{\Delta H + 1/2(V_g^2 - V_l^2)} \tag{7}$$

If the kinetic energy terms are neglected in the above equation, the result is that of an isenthalpic expansion and the quality is a function of temperature only.

By a chainge of variable the temperature T is made the independent variable instead of the distance z. Then Equations (1) through (6) may be solved by algebraic manipulations for dV_l/dT, dV_g/dT, dF_p/dT, and dF_w/dT in terms of the dependent variables V_l, V_g, V_p, and x; the parameters W and $\cos\theta$ and the physical and thermodynamic properties P, v_l, v_g, h, H, and ΔH which are functions of temperature only. The result is

$$\frac{dV_l}{dT} = \frac{-1}{V_l}\left\{\frac{dh}{dT} + \frac{\Delta H}{(1-x)}\frac{dx}{dT} + \frac{x}{(1-x)(\cos\theta\, V_g/V_p - 1)}\left[\frac{(V_g - V_l)^2}{2x}\frac{dx}{dT} + v_g\frac{dP}{dT} - \frac{dH}{dT}\right]\right\} \tag{8}$$

$$\frac{dF_w}{dT} = \frac{W}{V_l(V_p - \cos\theta\, V_g)}\left\{(V_p - \cos\theta\, V_g)\left[\Delta H\frac{dx}{dT} + (1-x)\frac{dh}{dT}\right] + (V_p - \cos\theta\, V_l)\left[x\frac{dH}{dT} - 1/2\,(V_g - V_l)^2\frac{dx}{dT}\right] + \left[\frac{\cos\theta\, V_l V_g}{W} - \frac{xv_g + (1-x)v_l}{A}V_p\right]\cdot A\left(\frac{dP}{dT}\right)\right\} \tag{11}$$

Combining Equations (1) and (2) with $A = a_g + a_l$ one obtains

$$V_g - \frac{Wx\,v_g\,V_l}{[AV_l - W(1-x)v_l]} \tag{12}$$

If x is considered a function of temperature only, one additional independent relation is needed along with proper boundary conditions for a solution of these differential equations to relate the dependent variables V_l, V_g, V_p, F_p, and F_w with temperature. The relation which was used is a modification of Linning's empirical relation and is

$$V_p = V_l\,[1 + (0.2/81)\,(T_o - T)^2] \tag{13}$$

In the range of this work, as will be discussed subsequently, it was found (*12*) that the solution of these annular flow equations, Equations (8) through (12), was not affected by the quality being assumed a function of temperature only, and further that the solution was insensitive to the choice of the equation to relate the interface velocity V_p with other dependent variables when a realistic range of values were allowed for V_p. Also $\cos\theta$ was taken as unity which was sufficiently accurate for the range of (L/D) ratios encountered here.

To relate the variables with distance along the pipe axis z it was postulated that the wall shear force could be related to z by using the usual friction factor–Reynolds number relation, with the Reynolds number given by $DV_l/\mu_l v_l$. The basis for this postulate was that the replacement of the relatively low velocity liquid core by a high velocity vapor core does not change the slope of the velocity distribution curve at the wall. Based on this consideration the following integral relation was obtained:

$$z = \int_{T_o}^{T}\left[\frac{D(1-\alpha)}{2fWV_l(1-x)}\cdot\frac{dF_w}{dT}\right]dT \tag{14}$$

where dF_w/dT is given by Equation (11).

The friction factor–Reynolds number relation was obtained from pressure drop, flow rate measurements for all liquid flow on the experimental equipment, and the data were represented by

$$f = 0.00180 + 0.125/(N_{Re})^{0.320} \tag{15}$$

Owing to the complexity of the equations a numerical solution was necessary and the method of Runge-Kutta (*13*) was used. A program was written (*14*) for a Burroughs-220 digital computer to facilitate the numerical solution. Physical and thermodynamic properties of water were obtained from the "Steam Tables" (*15*). This tabular data in the temperatures range from 170° to 330°F.

$$\frac{dV_g}{dT} = \frac{\cos\theta\, x\,(dH/dT) + 1/2\cos\theta\,(V_g^2 - V_l^2)\,(dx/dT) - xv_g(V_p/V_g)\,(dP/dT) - V_p(V_g - V_l)\,(dx/dT)}{x(V_p - \cos\theta\, V_g)} \tag{9}$$

$$\frac{dF_p}{dT} = \frac{[xv_g\,(dP/dT) - x(dH/dT) + 1/2\,(V_g - V_l)^2\,(dx/dT)]\,W}{(V_p - \cos\theta\, V_g)} \tag{10}$$

were fitted to within the accuracy of the data by least-square polynomials to be used in the computer program. Derivatives with respect to temperature of the physical and thermodynamic properties were obtained by differentiating the least-square polynomials. A check of the derivatives of the physical and thermodynamic properties was made by using two finite difference schemes (*16*), and agreement of 3 to 5% was found between the polynomial derivatives and the finite difference schemes.

Boundary conditions for the differential equations were taken at the point of initial vaporization where

$$T = T_o$$
$$V_l = V_o = Wv_o/A$$
$$V_p = V_o$$
$$x = 0$$

Difficulty was encountered as the point of initial vaporization is a singular point for Equations (8) and (12); that is they take the form zero over zero. Thus to start the numerical solution of the differential equations a trial-and-error determination of the initial slope $(dV_l/dT)_{T=T_o}$ was necessary as illustrated in Figure 2. When the solution was obtained for V_l as a function of T for a specified mass flow rate per unit area, inlet temperature, and outlet temperature, the corresponding tube length was computed by a Simpson's rule integration of Equation (14). As may be observed in Figure 2 six significant figures were required in this case (five to eight in general) to specify the initial slope to obtain a solution which satisfy the following physical considerations.

1. The vapor velocity is greater than the liquid velocity at every point other than the initial point in the expansion.

2. The vapor velocity is never negative or undefined at any point other than the initial point in the expansion.

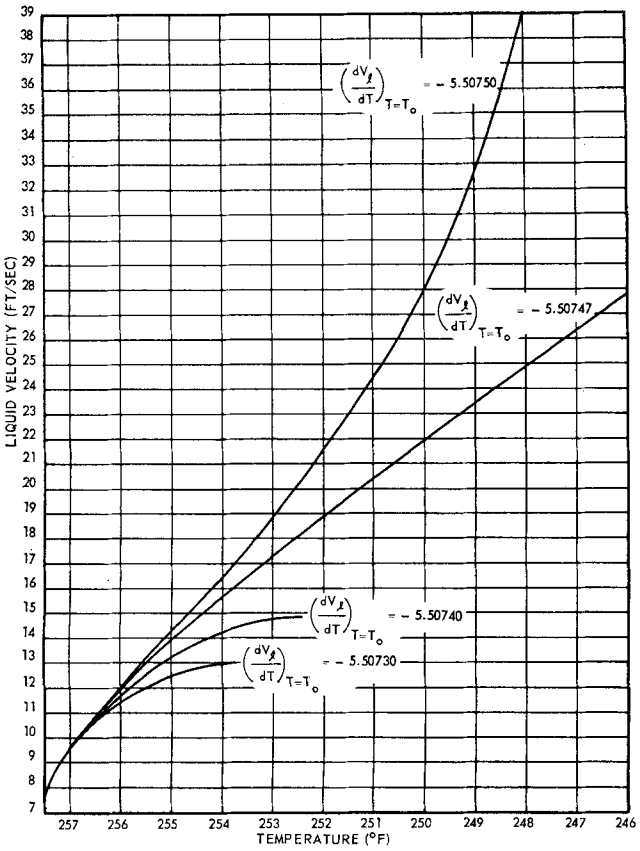

Fig. 2. Effect of $(dV_l/dT)_T = T_o$ on the solution of the annular flow equations.

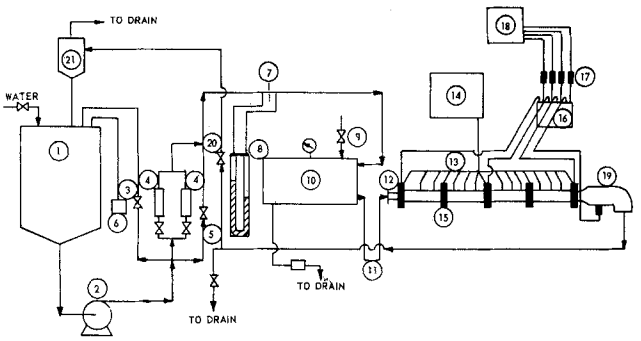

1. storage tank
2. pump
3. recycle control valve
4. rotameters
5. orifice control valve
6. potentiometer
7. metering orifice
8. manometer
9. steam control valve
10. heat exchanger
11. one inch loop
12. upstream observation section
13. thermocouples
14. temperature recorder
15. piezometric rings
16. constant temperature bath
17. pressure transducers
18. pressure recorder
19. expansion section
20. downstream control valve
21. cyclone separator

Fig. 3. Schematic diagram of the experimental system.

3. The liquid velocity V_l, the vapor velocity V_g, and the relative velocity factor $k = V_g/V_l$ must increase from the point of initial vaporization to the critical outlet temperature.

4. The slope of the liquid velocity vs. temperature curve dV_l/dT must approach zero at the critical outlet temperature.

The following inequality which bound V_l as a function of temperature only was obtained by examining Equation (12) on the basis of the first and second physical considerations:

$$\frac{W(1-x)v_l}{A} < V_l < \frac{Wxv_g}{A} + \frac{W(1-x)v_l}{A} \qquad (16)$$

Furthermore the fourth physical requirement was the basis for the method to predict critical flow. The critical flow was defined as the maximum flow rate for a given pressure at the point of initial vaporization and L/D ratio.

THE EXPERIMENTAL SYSTEM

The experimental system, shown schematically in Figure 3, was designed to obtain adiabatic, two-phase flow data for the system steam-water in a range where no data are presently available and to permit the determination of the accuracy of the annular flow model along with the assumptions on which the model is based.

With reference to Figure 3, water was pumped from the 125 gal. storage tank through the flow metering devices to a heat exchanger where the temperature was increased to a temperature which was slightly lower than the saturation temperature corresponding to the inlet pressure of the test section. Two-phase flow occurred at the point in the test section where the pressure corresponded to the saturation pressure at the liquid temperature. From the test section the two-phase mixture of steam and water flowed to the cyclone separator where the steam and water were separated.

The test section was 1.0 in. O.D. by 0.035 in. wall thickness 304 stainless steel seamless tubing 19.42 ft. long. The pressure was measured at the entrance, center, and exit of the test section and at the 3 in. I.D. glass expansion section by pressure transducers to within ± 0.5 lb./sq.in. The temperature was measured at sixteen equally spaced points along the test section by iron-constantan thermocouples which were previously calibrated to ± 1°F. The void fraction was measured at various test section cross sections to within the probable statistical error by the attenuation of a 1/16-in. diameter columniated beam of X-rays from a 45 Kvp. X-ray tube mounted on a traversing carriage. A detailed statistical analysis of the void fraction data was performed, and lucite mock-ups were used to establish that the spectrum of X-ray energy obtained from an X-ray tube could be used as a source of effective monoenergetic radiation (*17*). Complete details along with further data are to be published in a forthcoming paper.

DISCUSSION OF RESULTS

Experimental data were obtained for twenty-eight two-phase flow tests. The range of variables was mass flow rates per unit area, 445 to 864 lb./sq.ft.-sec.; inlet pressures, 32.4 to 66.5 lb./sq.in.abs.; discharge pressures, 25.9 to 56.5 lb./sq.in.abs.; and void fractions, 0.056 to 0.672.

Five assumptions were made in the derivation of the theoretical equations. The first assumption (horizontal tube) and the second assumption (steady state) were accomplished by the design and operation of the experimental system. The third assumption of the equality of velocities whether based on continuity, momentum, or energy is not strictly true but is probably not much in error in the highly turbulent flow as experienced in these tests. The fourth assumption of constant temperature and pressure at any section normal to the flow and the fifth assumption of thermodynamic equilibrium at all stages of the expansion would normally be expected to be approached unless the changes in temperature and pressure were so rapid that rates of heat and mass transfer became controlling. When the rates of heat and mass transfer become controlling, these two assumptions will not apply owing to the appearance of temperature gradients in the liquid and vapor phases. Results were obtained where these two assumptions did and did not apply. In Figure 4 a typical result is shown where the measured temperatures approach the saturation temperatures corresponding to the measured pressures along the tube which indicate that the fourth and fifth assumptions are applicable. Also in Figure 4 a typical result is shown where the measured temperatures do not approach the saturation temperatures

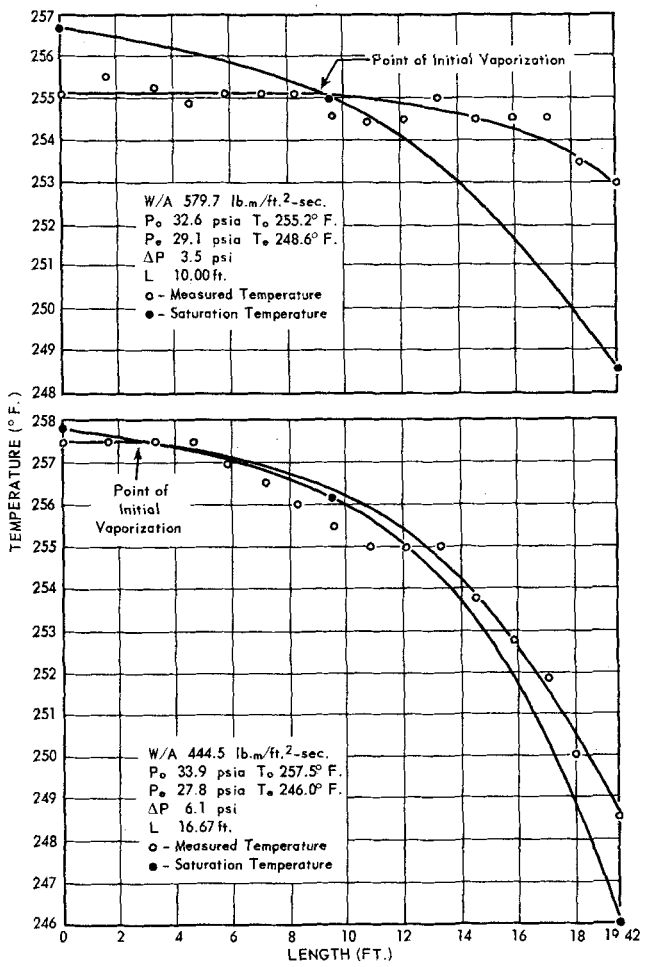

Fig. 4. Measured and saturation temperatures vs. axial tube length for adiabatic, two-phase flow.

corresponding to the measured pressures. For this test radial temperature gradients were large, and the fourth and fifth assumptions are not applicable. Consequently good agreement should be obtained between the annular flow equations and the experimental data when these assumptions are met, and correspondingly a deviation should be obtained between the theoretical equations and the experimental data when the assumptions are not met.

For the assumption that the wall shear force F_w could be related to z by using the usual friction factor–Reynolds number relation with $N_{Re} = DVi/\mu_{tvl}$, it will be seen that this approximation worked very well for the range of variables in this study. However if this assumption was not made, it would be necessary to approximate an average specific volume of the two-phase mixture and obtain a two-phase friction factor. Fauske (27) discussed the specific volume approximations used previously, presented a new one, and determined average two-phase friction factors for a study of critical steam-water flow in short tubes. Also Tek (28), among others (1, 3, 4), discussed this for two-phase flow in general, and he presented a two-phase, friction factor–Reynolds number correlation for gas-liquid flow. However these methods have not been as accurate as that obtained in this study as will be seen.

Comparisons were made of the computed void fraction with the measured void fractions and the computed tube lengths with the measured tube lengths for the thirteen tests where the measured temperatures approached saturation temperatures corresponding to the measured pressures. A comparison of the void fractions, measured and computed by the annular flow equations, showed that the computed void fractions were within the probable statistical error of the measured void fractions. By this comparison it was concluded that the annular flow equations described the complex phenomena to within the accuracy of the void fraction measurements. Since the void fraction measurement was hindered by the statistical error inherent in the measurement, a comparison of tube lengths computed from the annular flow equations with the experimentally measured tube lengths was also made. It was found that the maximum positive deviation was 7.9%, maximum negative deviation was −14.4%, and the average deviation was ± 5.2% for the thirteen runs. The individual comparisons are tabulated in reference 12 which contains the complete two-phase and single-phase flow data. It is to be noted that these deviations of the calculated values from the experimental values were generally random which would indicate that at least part of the lack of agreement between the experimental measurements and the computed values could be due to experimental error.

Also comparisons were made of the void fractions and tube lengths for the fifteen other runs where the measured temperatures were higher than the saturation temperatures corresponding to the measured pressures. Consequently radial temperature gradients existed in the two-phase flow nullifying the assumptions of constant temperature across any section normal to the flow and thermodynamic equilibrium at all stages of the expansion. Furthermore it was observed that the measured void fractions were less than the computed void fractions in all cases. The measured void fraction would be expected to be less than the computed void fraction, as a smaller fraction of the liquid had been vaporized compared with the fraction that would have been vaporized had thermodynamic equilibrium been attained at the cross section. Correspondingly the liquid velocity did not increase as rapidy as predicted by the annular flow equations as a result of the greater cross-sectional area for liquid flow and also as a result of the smaller interfacial shear forces. This would logically result in the measured tube length

being greater than the calculated tube length for an equal pressure drop. This was the case, and the computed values were from 17.9 to 44.3% less than the measured tube length, the average per cent deviation being 29.5% for the fifteen runs. These individual comparisons are also tabulated in reference *12*.

Hatch and Jacobs (*18*), Houghton (*19*), and Anderson, Haselden, and Mantzouranis (*20*) have also observed or studied the phenomenon of a temperature gradient in the liquid annulus of two-phase flow of a pure fluid.

It would be desirable if definite limits could be placed on the variables of mass flow rate per unit area and inlet pressure to bound the regions in which the annular flow equations would hold. This is not presently possible owing to the complex flow situation. However generally higher mass flow rates per unit area were experienced when heat and mass transfer rates became controlling. This would be expected as liquid residence time is longer and the liquid film becomes thinner for lower mass flow rates, thus permitting thermodynamic equilibrium to be approached more closely. In general it is concluded that if the annular flow equations are used for design purposes to compute the two-phase flow pressure drop for a given mass flow rate and tube length, the computed pressure drop will be accurate to at least ± 10% if thermodynamic equilibrium is approached. If thermodynamic equilibrium is not approached, the computed pressure drop will be of the order of 15 to 45% greater than the actual pressure drop, depending upon the departure from thermodynamic equilibrium. Thus the use of the annular flow equations will give inherent overdesign rather than inherent underdesign.

EFFECT OF INTERFACE VELOCITY RELATIONS ON THE SOLUTION OF THE ANNULAR FLOW EQUATIONS

As previously mentioned the solution of the annular flow equations was found to be insensitive to the relation for the interface velocity when a realistic range of values were allowed for V_p. To illustrate this fact two additional relations for V_p, $V_p = V_l$, and $V_p = 1.2\ V_l$ were used in place of Equation (13) in the solution of the annular flow equations and represent a range of probable values for V_p. For the thirteen runs where assumptions for the equations were met the average per cent deviations in comparing computed tube lengths with measured tube lengths using the latter relation was 7.1% and using the former was 14.6%. From these considerations it may be concluded that equation (13) more aptly described the physical situation but not significantly better than the two above relations for V_p.

Also it was found for the range of this work the solution of the annular flow equations was unaffected by neglecting the kinetic energy terms in the total energy equation, Equation (7). Solutions were obtained using and omitting the kinetic energy terms with essentially the same results being obtained.

COMPARISON OF FLOW MODELS

The pressure drops as computed by the homogenous flow model (*6*), the Martinelli-Nelson model (*5*), and the annular flow equations were compared for the thirteen runs where the assumptions of thermodynamic equilibrium at all stages of the expansion and constant temperature across any section normal to the flow were met, as these are required for all three models. The individual comparisons for each of the thirteen runs are tabulated in reference *12*.

The Martinelli-Nelson model predicted pressure drops which were consistently higher than the experimental pressure drops. Consistently high values resulted from the ratio $(\Delta P_{TPF}/\Delta P_o)$ being too large. $(\Delta P_{TPF}/\Delta P_o)$ is the ratio of the frictional pressure drop for two-phase flow to the frictional pressure drop for single-phase flow with both flows at the same conditions of temperature and pressure. It is a function of the mean pressure of the system and the exit quality. The failure of the Martinelli-Nelson model to describe the pressure drop accurately was to be expected, since the model was based on results from isothermal two-component pressure drop data. The authors stated in their paper that the method was a tentative method for rapid calculation which was based upon a meager amount of data and required further experimental verification before it could be considered valid. The data on which the model was based covered a range of 18 to 3,000 lb./sq. in. abs. and exit qualities of 4 to 100%. The accepted limit of accuracy of the Martinelli-Nelson model is ± 40%, and it was found that most of the pressure drop results as calculated by the Martinelli-Nelson model were within this range, the average per cent error being 46.5% for the thirteen runs.

The homogenous flow model was more successful in predicting the two-phase flow pressure drop, and the average per cent error for this model was 23.8% for the thirteen runs.

The average per cent error for the annular flow equations was 7.3% as compared with 23.8% for the homogenous flow model and 46.5% for the Martinelli-Nelson model. On the basis of these results it is concluded that the homogenous flow model and the Martinelli-Nelson model will give approximate results involving relatively simple calculations, while the annular flow equations will give results of the order of ± 10% and less but involve complicated calculations. In order to eliminate these complicated calculations design charts for the system steam-water have been prepared from the numerical solution of the annular flow equations. These design charts are presented in the next section.

DESIGN CHARTS

In Figures 5, 6, and 7 design charts are presented for the system steam-water to permit the rapid computation of two-phase flow parameters. These design charts are based on the numerical solution of the annular flow equations for even intervals of mass flow rate and inlet pressure. The range of the charts is inlet pressure, 30 to 150 lb./sq. in. abs.; mass flow rate, 300 to 1,000 lb.$_m$/sq. ft.-sec.; and L/D ratio, 25 to 1,000. This represents an extrapolation of the range of variables, as experimental verification has been obtained in this work for inlet pressures from 32.4 to 66.5 lb./sq. in. abs., discharge pressures from 25.9 to 56.5 lb./sq. in. abs., mass flow rates from 444.5 to 763.6 lb.$_m$/sq. ft.-sec., and L/D ratios from 135.5 to 250.6. It is felt that this extrapolation is justified to facilitate comparisons of the model with any forthcoming data, as a minimum of 10 min. computing time is required on a high-speed digital computer to obtain a solution to the equations for a given mass flow rate and inlet pressure. Also for the design engineer it supplies an additional and probably more accurate method to estimate flow variables.

In Figure 5 the pressure at any point in the tube is given as a function of the L/D ratio up to the critical L/D ratio $(L/D)_c$ with mass flow rate as a parameter. In Figure 6 the mass flow rate is given as a function of $(L/D)_c$ with inlet pressure as a parameter. In Figure 7 the critical outlet pressure is given as a function of mass flow rate with inlet pressure as a parameter. With Figure 5 the pressure drop can be obtained for a given inlet pressure, flow rate, and L/D ratio including the $(L/D)_c$. For a specified mass flow rate and inlet pressure the $(L/D)_c$ may be obtained from Figure 6 and the corresponding

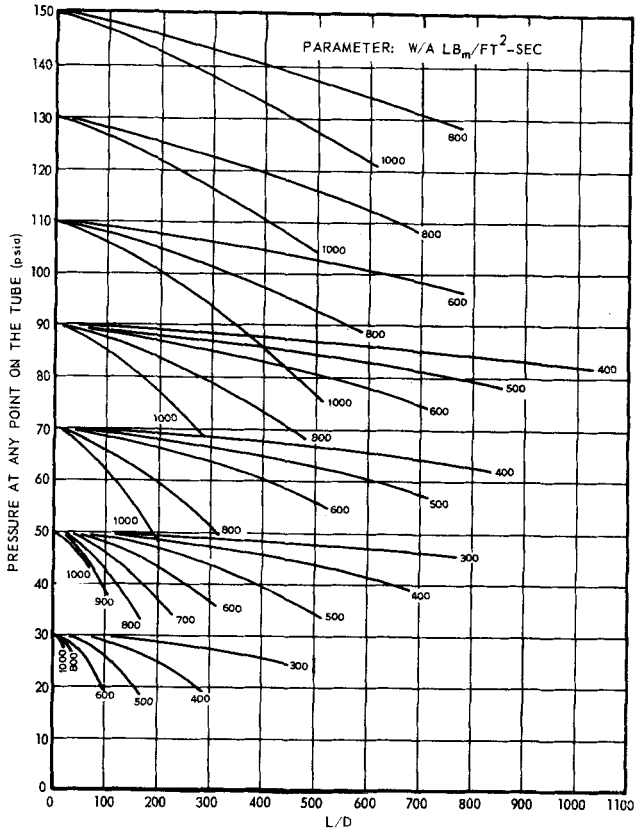

Fig. 5. Pressure at any point in the tube vs. L/D ratio for the system steam-water.

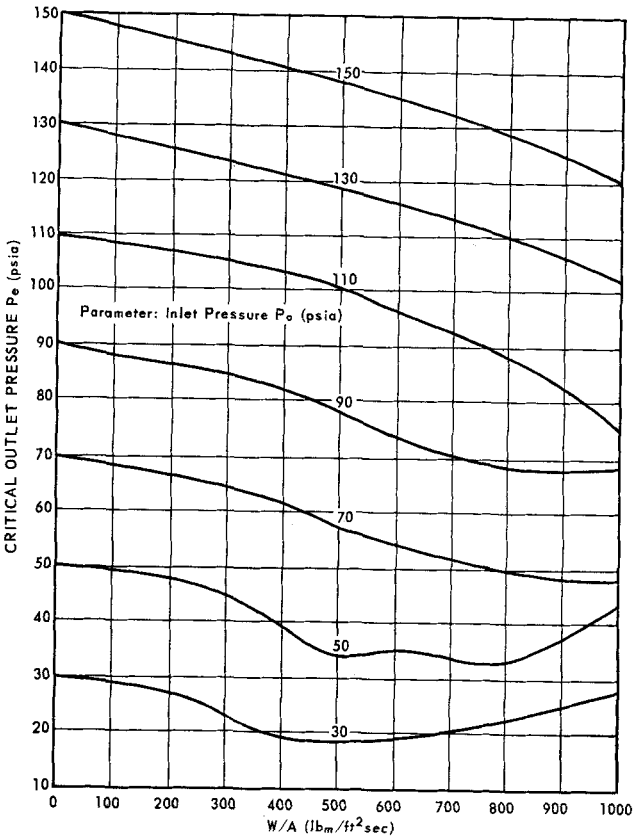

Fig. 7. Critical outlet pressure vs. mass flow rate for the system steam-water.

critical outlet pressure obtained from Figure 7. It should be noted that the results presented in Figure 7 are independent of any friction factor—Reynolds number relation. However the results presented in Figures 5 and 6 are based on Equation (15).

It should be further noted that the results given in Figure 7 are the locus of critical outlet pressures obtained from Figure 5 plotted as a function of mass flow rate per unit area. Concerning the minimum in the critical outlet pressure for the lower inlet pressures, it may be reasoned intuitively as one limiting case, that of the critical outlet pressure equaling the inlet pressure for zero mass flow rate per unit area with an infinitely large $(L/D)_c$ ratio, and as the other limiting case, that of the critical flow of saturated water through an orifice where $(L/D)_c$ approaches zero. Thus it would follow that the critical outlet pressure could pass through a minimum for a given inlet pressure as the $(L/D)_c$ ratio decreased from a very large number to essentially zero.

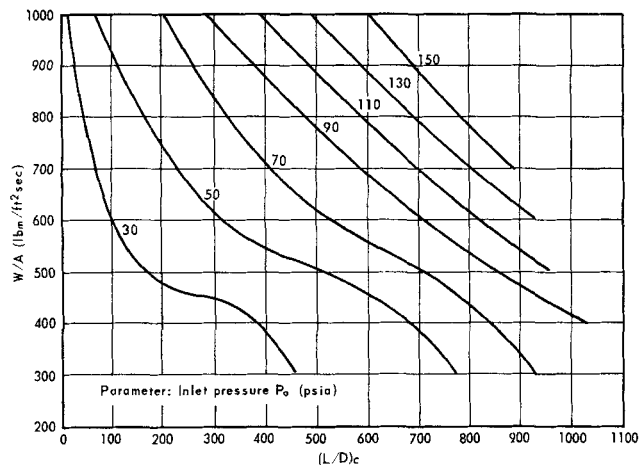

Fig. 6. Mass flow rate vs. $(L/D)_c$ for the system steam-water.

COMPARISON WITH PREVIOUS WORK

Data from previous investigations of the adiabatic two-phase flow of steam and water are for critical flow only. The data of Benjamin and Miller (6) were taken from cascade drain lines of a power plant over a range of inlet pressures from 20.0 to 35.8 lb./sq. in. abs. and mass flow rates from 157 to 286 lb.$_m$/sq. ft.-sec. The average per cent deviation of the critical outlet pressure computed from the annular flow equations from the experimental critical outlet pressures was —20.6%. Isbin (24) also reported that his data were significantly lower than Benjamin and Miller's data.

For Bottomley's (21) one run at 260 lb.$_m$/sq. ft.-sec., inlet pressure 41.0 lb./sq. in. abs., and outlet pressure 22.0 lb./sq. in. abs. the outlet pressure predicted by the annular flow equations was 61.5% higher than the measured value. Isbin (24) reported Bottomley's measured value was lower than the value he observed also.

Burnell (22) reported nine experimental runs. For four runs at inlet pressures of 158, 114, 52.4, and 24.0 lb./sq. in. abs. the predicted critical outlet pressures from the annular flow equations differed by 57, 54, 31, and 9%, respectively. The inlet pressures for Burnell's five other runs were 14.3 lb./sq. in. abs. and less which is less than the lower limit of accuracy of the least-square polynomials fitted to the thermodynamic properties, and no comparison could be made. Isbin (24) found that his data were within ± 10% of Burnell's data in the exit pressure range of 6 to 15 lb./sq. in. abs. and 20 to 35% lower in the exit pressure range 24.5 to 58.5 lb./sq. in. abs.

Linning reported twelve experimental runs in ⅛-in. diameter tube for ranges of inlet pressures from 20.8 to

29.8 lb./sq. in. abs., mass flow rates from 266 to 485 lb.$_m$/sq. ft.-sec., and tube lengths from 7.2 to 30.0 in. The average per cent deviation of the critical outlet pressure computed from the annular flow equations from the experimental values was 21.4%. Isbin (*24*) found the data of Linning to be 40 to 50% less than his experimental values.

Isbin (*24*) obtained critical, two-phase flow data of steam and water in the range of critical outlet pressure from 4 to 43 lb./sq. in. abs. and exit qualities from 1.0 to 100% by mixing steam and water and flowing the mixture through short tubes and annular test sections. Isben reported extensive data for exit qualities more than 3%, while only three values were reported for exit qualities less than 3%. (Exit qualities greater than 3% require heat transfer to the flow starting from the point of initial vaporization.) Results of the solution of the annular flow equations from the design charts were compared with this data and found to agree within 17%.

Recently three other studies were performed, those of Faletti and Moulton (*25*), Zaloudek (*26*), and Fauske (*27*), who used the same technique employed by Isbin of mixing steam and water and flowing the mixture through short tubes. All of Faletti and Moulton's data were for mass flow rates per unit areas greater than 1,000 lb.$_m$/sq. ft.-sec. for qualities less than 3%, out of the range of the design charts. However extrapolating for the two runs at 1,062 lb.$_m$/sq. ft.-sec. agreement was 15 and 19%. Only one run of Zaloudek's was less than 1,000 lb.$_m$/sq. ft.-sec. at an exit quality less than 3%, and the exit quality predicted by the annular flow equations was within 4% of this experimental value. Unfortunately no comparison could be made with Fauske's data as all mass flow rates per unit area reported were over 1,000 lb.$_m$/sq. ft.-sec. for exit qualities less than 3%. For a detailed comparison of these four works (*24, 25, 26, 27*) refer to Zaloudek's paper (*26*).

CONCLUSIONS

The following conclusions are made on the basis of the results of this study.

1. The adiabatic, two-phase flow of steam and water in a horizontal tube from the point of initial vaporization to the exit of the tube was successfully described by the annular flow equations when the basic assumptions of thermodynamic equilibruim at all stages of the expansion and constant temperature across any section normal to the flow were approached. The accuracy in computing the two-phase flow pressure drop by the annular flow equations for a specified mass flow rate, inlet pressure, and tube length was ± 10% when these basic assumptions were met.

2. When the basic assumptions of thermodynamic equilibrium at all stages of the expansion and of constant temperature across any section normal to the flow were not approached, the pressure drop which was predicted from the annular flow equations was from 15 to 45% greater than the measured pressure drop.

3. The solution of the annular flow equations required that only the initial conditions of mass flow rate and inlet pressure be known along with the tube length or outlet pressure. Further information concerning the flow variables at some point downstream from the point of initial vaporization was not required to obtain a solution for the flow variables as a function of distance along the tube. All previous flow models have required additional information about the flow variables at some point downstream from the point of initial vaporization or have required that a simplifying assumption be made to obtain a solution.

ACKNOWLEDGMENT

The aid of the Dow Fellowship to R. W. Pike by the Dow Chemical Company is gratefully acknowledged. The authors are grateful to Mrs. Maudine Smith for her assiduous effort in preparing the manuscript, and to Humble Oil & Refining Company for assistance in publishing the work.

NOTATION

A = tube cross-sectional area, sq. ft.
a_g = cross-sectional area of vapor phase, sq. ft.
a_l = cross-sectional area of liquid phase, sq. ft.
D = tube diameter, ft.
F_p = interface shear force, lb.$_f$
F_w = wall shear force, lb.$_f$
f = friction factor, dimensionless
g_c = conversion factor 32.174, ft.-lb.$_m$/sec.^{2}-lb.$_f$
H = enthalpy of vapor, B.t.u./lb.$_m$
h = enthalpy of liquid, B.t.u./lb.$_m$
L = tube length, ft.
L/D = tube length to diameter ratio, dimensionless
$(L/D)_c$ = critical tube length to diameter ratio, dimensionless
P = pressure, lb./sq. in. abs.
N_{Re} = Reynolds number, dimensionless
T = temperature, °F.
T_e = exit temperature, °F.
T_o = inlet temperature, °F.
V = velocity, ft./sec.
V_g = vapor velocity, ft./sec.
V_l = liquid velocity, ft./sec.
V_p = interface velocity, ft./sec.
v = specific volume, cu. ft./lb.$_m$
v_g = specific volume of vapor, cu. ft./lb.$_m$
v_l = specific volume of liquid, cu. ft./lb.$_m$
W = total mass flow rate, lb.$_m$/sec.
W/A = total mass flow rate per unit area, lb.$_m$/sq. ft.-sec.
x = quality, dimensionless
z = distance along tube axis, ft.

Greek Letters

α = void fraction, defined as a_g/A, dimensionless
θ = angle formed by the tube axis and the vapor-liquid interface, rad.
μ_l = liquid viscosity, centipoise
ρ = density, lb.$_m$/cu. ft.
ρ_g = vapor density, lb.$_m$/cu. ft.
ρ_l = liquid density, lb.$_m$/cu. ft.

Subscripts

c = critical
e = exit conditions
g = vapor
l = liquid
o = initial conditions or all liquid flow
p = interface

LITERATURE CITED

1. Gresham, W. A., P. A. Foster, and R. J. Kyle, *WADC Rept. No. 55-422*, Part 1, ASTIA Document No. AD-95, 752 (June, 1955).
2. Ward, H. C., J. E. Rhodes, W. T. Ziegler, and L. W. Ross, *WADC Rept. No. 59-230* (August, 1959).
3. Isbin, H. S., R. H. Moen, and D. R. Mosher, *Rept. No. AECU-2994*, U.S. Atomic Energy Commission (November, 1954).
4. Bennett, J. A. R., *Atomic Energy Research Establishment Rept. No. AERE CERI-2497* (March, 1958).
5. Martinelli, R. C., and D. B. Nelson, *Trans. Am. Soc. Mech. Engrs.*, **70**, 695 (1948).
6. Benjamin, M. W., and J. G. Miller, *ibid.*, **64**, 657 (1942).

7. Lockhart, R. W., and R. C. Martinelli, *Chem. Eng. Progr.*, **45**, No. 1, pp. 39-48 (1949).
8. Linning, D. L., Ph.D. thesis, University of Glasgow, Glasgow, Scotland (1951).
9. Charvonia, D. A., *Armed Services Technical Information Agency Document AD-208,040, Project Squid Tech. Rept. PUR-32-R* (December, 1958).
10. Jens, W. H., and G. Leppert, *J. Am. Soc. Naval Engrs.*, **67**, 137, 437 (1955).
11. Rodabaugh, Rowena, *Two-Phase Flow and Acoustic Phenomena in Gases and Liquids: Literature Search No. 177*, Jet Propulsion Laboratory, California Institute of Technology, Pasadena, California (June, 1960).
12. Pike, R. W., Ph.D. thesis, Georgia Inst. Technol., Atlanta, Georgia (1962).
13. Kuntz, K. S., "Numerical Analysis," Chap. 7, McGraw-Hill, New York (1957).
14. "A Reference Manual: Burroughs Algebraic Compiler," Burroughs Corporation, Detroit, Michigan.
15. Keenan, J. H., and F. G. Keyes, "Thermodynamic Properties of Steam," Wiley, New York (1956).
16. Pike, R. W., Ph.D. thesis, p. 39, Georgia Inst. Technol., Atlanta, Georgia (1962).
17. *Ibid.*, p. 60.
18. Hatch, M. R., and R. B. Jacobs, *A.I.Ch.E. Journal*, **8**, No. 1, pp. 18-25 (1962).
19. Houghton, Gerald, *Nuclear Sci. and Eng.*, **12**, 390-397 (1962).
20. Anderson, G. H., G. G. Haselden, and B. G. Mantzouranis, *Chem. Eng. Sci.*, **16**, 222-230 (1961).
21. Bottomley, W. T., *Trans. North East Coast Inst. Engrs. and Shipbuilders*, **53**, 65-100 (1936-1937).
22. Burnell, J. G., *Eng.*, **164**, 752 (1947).
23. Linning, D. L., Ph.D. thesis, p. 207, Univ. Glasgow, Glasgow, Scotland (1951).
24. Isbin, H. S., J. E. Moy, and A. J. R. Da Cruz, *A.I.Ch.E. Journal*, **3**, 361 (1957).
25. Faletti, D. W., and R. W. Moulton, *ibid.*, **9**, 247-253 (1963).
26. Zaloudek, F. R., *HW-68934* (March, 1961).
27. Fauske, H. K., *ANL-6633* (Oct., 1962).
28. Tek, M. R., "Handbook of Fluid Dynamics," Sect. 17, McGraw-Hill, New York (1961).

Manuscript received November 5, 1962; revision received August 5, 1963; paper accepted August 8, 1963. Paper presented at A.I.Ch.E. New Orleans meeting.

Single-Particle Studies of Ion Exchange in Packed Beds: Cupric Ion-Sodium Ion System

M. GOPALA RAO and M. M. DAVID

University of Washington, Seattle, Washington

Considerable work has been expended on the development of analytical methods for predicting the performance of ion-exchange materials in packed beds. The resulting methods however have had only limited utility for design purposes because the physical and mathematical complications of the problem have necessitated use of various simplifying assumptions which have restricted the general applicability of the methods. Numerical techniques with high-speed computers offer a potential means for handling the mathematical complications of packed-bed systems without resort to undue simplifying assumptions. To use these techniques though, adequate models for the process and values for the rate constants included in these models must be available. These requirements demand in turn an extensive body of data for ion exchange in packed beds, both to verify proposed or suggest new models and to obtain generalized correlations for the rate constants in the models. The present study was undertaken to supply such data by an intensive investigation over a wide range of operating conditions of the exchange rate of copper ions for sodium ions on a typical cation exchanger, Dowex 50W-X8. Choice of this system was based on the relative sparsity of comprehensive rate data for the exchange of ions with unequal valences (especially in concentrated solutions), the extensive equilibrium data available for the system (23), the suitability of the system for the experimental procedure, and industrial interest in the system (23). Ion exchange of copper for sodium has been studied in dilute solutions by Selke and Bliss (21), but extensive rate studies of this system are lacking.

M. Gopala Rao is at Gonzaga University, Spokane, Washington.

CURRENT CONCEPTS

Although ion exchange is essentially a metathical process which for the reaction of this study can be written as $Cu_r + 2Na_s \rightleftarrows Cu_s + 2Na_r$ (r and s denote the exchanger and external solution phases, respectively), the rates of ion exchange are determined by the mass transfer steps in the process. For the modern ion exchangers which are usually produced as small porous particles, the overall rate of exchange is controlled either by the resistance to mass transfer between the external fluid and the exchanger surface, by the resistance to mass transfer within the particle, or by the combination of these two resistances. As in other interphase transfer processes equilibrium is considered to exist between the two phases at the boundary formed by the exterior surface of the particle.

In packed beds of ion-exchange materials mass transfer from the bulk solution to the exchanger surface is effected by both convection and ionic diffusion. The rate of mass transfer for this step has usually been described in design